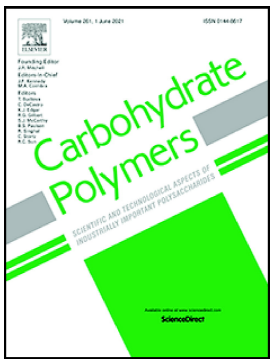

In-situ encapsulation and construction of Lac@HOFs/hydrogel composite for enhancing laccase stability and azo dyes decolorization efficiency

Xue Yang, Fei Shi, Xiaolei Su, Artur Cavaco-Paulo, Hongbo Wang, Jing Su

PII: S0144-8617(23)00622-7

DOI: https://doi.org/10.1016/j.carbpol.2023.121157

Reference: CARP 121157

To appear in: *Carbohydrate Polymers*

Received date: 26 March 2023

Revised date: 21 June 2023

Accepted date: 26 June 2023

Please cite this article as: X. Yang, F. Shi, X. Su, et al., In-situ encapsulation and construction of Lac@HOFs/hydrogel composite for enhancing laccase stability and azo dyes decolorization efficiency, *Carbohydrate Polymers* (2023), https://doi.org/10.1016/j.carbpol.2023.121157

In-situ encapsulation and construction of Lac@HOFs/hydrogel composite for enhancing laccase stability and azo dyes decolorization efficiency

Xue Yang [a], Fei Shi [a], Xiaolei Su [a], Artur Cavaco-Paulo [a,b], Hongbo Wang [a*], Jing Su [a,b*]

[a] Jiangsu Engineering Technology Research Centre of Functional Textiles, Jiangnan University, Wuxi 214122, China

[b] Centre of Biological Engineering, University of Minho, Campus de Gualtar, 4710-057 Braga, Portugal

E-mail addresses: sujing@jiangnan.edu.cn (J. Su); wxwanghb@jiangnan.edu.cn (H. Wang).

*Corresponding Author:

Jing Su, sujing@jiangnan.edu.cn

Hongbo Wang, wxwanghb@jiangnan.edu.cn

Abstract

Enzymes with high catalytic activity and stability have been used for the sustainable development of green chemical applications, such as water remediation. Immobilized laccase can be used to construct a synergistic system for adsorption and degradation, which has great potential for water remediation. Herein, a hydrogen-bonded organic framework was installed onto laccase *in-situ* to form a net-carboxylate-arranged defective cage, which enhanced its catalytic stability. Thereafter, the CMC/PVA/Lac@HOF-101 hydrogel was fabricated by freeze–thaw cycles using sodium carboxymethylcellulose and polyvinyl alcohol as carriers and copper (II) as a cross-linker. Notably, the MOFs/hydrogel as a protective carrier of laccase maintain long-term recyclability and catalytic stability. After the fifth catalytic cycle, approximately 66.7 %

activity of the CP-Lac@HOF-101 was retained. When both free laccase and CP-Lac@HOF-101 were used for decolorization of Acid Orange 7 (AO), the removal rates were 10.9 % and 82.5 % after 5 h, respectively. Furthermore, even in the presence of metal cations, almost 60.0 % of the AO removal efficiency was achieved. The relationship between the structure of the azo dyes and decolorization efficiency of the synergistic system was further investigated. This study offers a method for constructing enzyme@HOF-based composite hydrogels and provides a promising water remediation strategy.

Keywords: Laccase immobilization; Hydrogen-bonded organic framework; Hydrogel composite; Water remediation

1. Introduction

With rapid industrialization, water pollution has become a global problem (Pierrat et al., 2023; Slama et al., 2021). Ongoing emissions of dye-containing wastewater have threatened human health and natural ecosystems in recent decades (Solayman et al., 2023). Azo dyes are the most widely used dyes in the textile industry, in which the substituted aromatic structure is linked using one or more azo bridges (N=N) (Malik & Müller, 2016). Because of their genotoxic, carcinogenic, xenobiotic, and recalcitrant nature, the discharge of azo dyes effluents can lead to serious water pollution and threaten human health (Bokare, Chikate, Rode, & Paknikar, 2008; Ghaheh et al., 2021). Therefore, many advanced technologies have been used for water remediation, including physisorption (Hasan, Shenashen, Hasan, Znad, & Awual, 2021), oxidation processes (Rajoriya, Bargole, George, & Saharan, 2018; D. Wang, Zhu, et al., 2021), electrocatalysis (Xiao et al., 2016), and microbiological methods (Kurade, Waghmode, Patil,

Jeon, & Govindwar, 2017; Yuan et al., 2023). The enzymatic degradation of azo dyes will be an ideal solution as they are highly specific catalysts that produce byproducts of lower toxicity. Laccase, an oxidoreductase, exhibits high efficiency and wide substrate diversity, with water being the only byproduct of the catalytic process. Therefore, laccase has attracted considerable attention for their use in the degradation of organic pollutants. (Su, Fu, Wang, Silva, & Cavaco-Paulo, 2018). Iark et al. isolated a new laccase from *Oudemansiella canarii* that could degrade 80 % of Congo red dyes within 24 h (Iark et al., 2019). However, the non-recyclability and poor stability of laccase have discouraged its practical application. Laccase is prone to losing its activity in response to external stimuli, such as elevated temperatures, extreme pH, and non-aqueous solutions (Backes et al., 2021). Therefore, enzymes immobilization has emerged as a method for generating stable and reusable biocatalysts.

Over the past decade, porous materials, including mesoporous silica and porous organic frameworks (POFs), have been developed as carriers for most materials (Dong, Wee, Peh, & Zhao, 2021; Feng et al., 2022; Huang, Chen, & Ouyang, 2022; Kitagawa, 2017). Wang et al. first immobilized laccase onto presynthesized magnetic mesoporous silica nanoparticles via metal-affinity adsorption. However, this method inherently relies on the adsorption and diffusion rates of laccase (F. Wang, Guo, Yang, & Liu, 2010). POFs are porous materials with diverse topologies, and include metal-organic frameworks (MOFs), covalent organic frameworks (COFs), and hydrogen-bonded organic frameworks (HOFs). The immobilization of laccase with *in-situ* growth of POFs prevents enzymes leaching, and the substrate could diffuse into the POFs and arrive at the active site of laccase (Xin Li et al., 2020). However, the laccase encapsulation by

MOFs and COFs must remain under aqueous conditions or at room temperature, which inhibits the development of these materials (Chen et al., 2022; Lin & Chen, 2019). HOFs are another class of porous materials assembled by weak intermolecular interactions of hydrogen bonds. Compared to the MOFs and COFs synthesis processes, the crystallization process of HOFs is much milder, and high pressure and temperature or strong acidity are not required. HOFs are metal-free structures with low biotoxicities and good biocompatibilities (Tang et al., 2021; Yang et al., 2023). Hence, the distinct linkage topology of HOFs, with surprisingly stable and permanently porous structures, has been demonstrated to act as carriers for encapsulated enzymes. Liang et al. encapsulated the enzymes with HOFs, which were constructed using water-soluble tetra-amidinium and tetracarboxylate (Liang et al., 2019). The crystalline coating of HOFs offers protection for enzymes, and hence, enhances their durability in various interfering environments. Tang et al. encapsulated the proteins *in-situ* in HOFs for enzymes catalysis in living cells (Tang et al., 2021). This method of *in-situ* encapsulation of laccase via HOFs showed solution processability and simple generation, which may accelerate the large-scale industrialization of biocatalysis. Notwithstanding all these advantages, the powder form of POFs is difficult to reclaim from dye-containing wastewater, which limits their applications (S. Li & Huo, 2015; Peng et al., 2021). Hence, combining POFs with functional substances or matrix materials to form POF-based composites has attracted considerable attention. Hydrogels with three-dimensional polymer network structures have shown advantages, such as non-toxicity, low toxicity, and excellent biocompatibility. Hydrogels have attracted considerable attention as promising materials for POFs encapsulation (Miao et al., 2022).

Sodium carboxymethylcellulose (CMC) is a high-performance biocarrier because of its hydrophilicity, biocompatibility, and biodegradability. Usually, an immobilized carrier for laccase possesses a certain mechanical strength; however, pure CMC hydrogels exhibit weak elasticity. Mixed CMC components with good mechanical properties can overcome these limitations. Poly(vinyl alcohol) (PVA) is a suitable option because of its excellent mechanical properties and biocompatibility. Yang et al. synthesized a spherical aerogel using CMC and PVA composite polymers as the matrix and MIL-101 (Cr) as the filler (C. Yang, H. R. Yang, Q. D. An, Z. Y. Xiao, & S. R. Zhai, 2022). The CMC/PVA/MIL-101 aerogel effectively captured heavy metal ions from wastewater. Javanbakht et al. fabricated porous materials for growing MOF in CMC to achieve a carrier system for prolonged drug release manner(Javanbakht, Pooresmaeil, & Namazi, 2019). However, the application of CMC/PVA and POFs as enzymes carriers for wastewater treatment has rarely been studied.

Inspired by this, laccase was encapsulated in HOF-101 (Lac@HOF-101), which was synthesized via a biomimetic mineralization process. Thereafter, CMC and PVA as carriers, Lac@HOF-101 as a biocatalyst, copper (II) as a cross-linking agent to lock the aligned macromolecules, and the CMC/PVA/Lac@HOF-101 hydrogel (CP-Lac@HOF-101) were prepared via freeze-thaw cycles. Lac@HOF-101 and CP-Lac@HOF-101 were also prepared and characterized. Acid Orange 7, an azo dye, was further explored as a target pollutant to demonstrate the adsorption and degradation performance of CP-Lac@HOF-101. In addition, some key factors were investigated in detail during the decolorization process, such as the temperature, concentration of the substance, and presence of interfering cations. Furthermore, adsorption and enzymatic reaction mechanisms for

synergistic degradation were proposed and validated.

2. Materials and methods

2.1. Materials

Laccase was purchased from Sigma-Aldrich Chemical Co., Ltd. (*Trametes versicolor*; St. Louis, MO, USA). N, N-Dimethylformamide (DMF), copper (II) nitrate hydrate, methanol (MeOH), sodium carboxymethylcellulose (CMC; USP grade, degree of substitution: 0.7, viscosity: 300–800 mPa·s, 2 % in H_2O at 20 °C), poly(vinyl alcohol) (PVA, degree of polymerization: 1700, degree of alcoholysis: 88 %), sodium chloride (NaCl), potassium chloride (KCl), magnesium chloride ($MgCl_2$), and calcium chloride ($CaCl_2$) were purchased from Sinopharm Chemical Reagent Co, Ltd. (Shanghai, China). 4,4',4'',4'''-(1,9-dihydropyrene-1,3,6,8-tetrayl) tetrabenzoic acid (H4TBAPy), 2, 2'-azino-bis (3-ethylbenzothiazoline-6-sulfonic acid) (ABTS), and Acid Orange 7 (AO) were obtained from InnoChem Science & Technology Co., Ltd. (Beijing, China). The correlation between the concentration of AO dye and its absorbance is shown in Tab. S1 and Fig. S1.

2.2 Preparation of the materials

Synthesis of HOF-101: HOF-101 was synthesized according to the method previously described by Chen et al. (Chen et al., 2021). H4TBAPy (150 mg), as an organic linker, was dissolved in 22.5 mL DMF. MeOH was added, and the mixture was stirred for 1 min (90 mL, 25 ℃). The mixed solution was aged for 24 h. Finally, HOF-101 was collected by centrifugation (1000 × g, 25 min) and washed with deionized (DI) water.

***In-situ* installation of HOF-101 onto laccase:** Lac@HOF-101 was synthesized via a

biomimetic mineralization process. H4TBAPy (10 mg) was dissolved in 1 mL DMF. Laccase was dissolved in 9 mL DI water. These solutions were then mixed and stirred at room temperature for 10 min. Lac@HOF-101 was collected by centrifugation (1000 × g, 25 min) and washed with DI water. Biocomposite was obtained by vacuum freeze-drying and stored at 4 °C for further structural analysis.

Synthesis of CMC/PVA and CMC/PVA/Lac@HOF-101 hydrogel: PVA powder (0.9 g) was dissolved in 10 mL DI water at 95 °C, with stirring. CMC (0.45 g) and Lac@HOF-101 were mixed in 15 mL DI water with constant stirring for 1 h to obtain a homogeneous solution. The PVA solution was slowly added to the prepared CMC/Lac@HOF-101 solution and stirred at 250 rpm for 30 min. After degassing via sonication for 1 h, clear solutions were obtained. The clear solutions were then poured into polystyrene dishes (100 and 200 mm in diameter) and frozen at -20 °C for 24 h. A copper nitrate trihydrate solution (1.0 M, 50 mL) was prepared by dissolving it in DI water. Subsequently, the frozen samples were transferred to 25 °C and 1.0 M Cu $(NO_3)_2 \cdot 3H_2O$ solutions were added, where the ice melted over time. The CMC/PVA/Lac@HOF-101 hydrogel (CP-Lac@HOF-101) was then subjected to vacuum-free drying for subsequent use. For comparison, the above steps replicated immobilized laccase with free laccase or no added laccase (named CP-Lac and CP, respectively).

2.3. Materials characterization and measurements

The materials characterization and measurements are provided in **Supplementary Information**.

2.4. Statistical analyses

Enzyme activity assays were performed in triplicate for each sample. The highest activity was

considered as 100 % and the outcomes were transformed into relative activities. The decolorization efficiency was measured in triplicate for each sample, and the percentage of color removal was analyzed using a UV−vis spectrophotometer to record the characteristic absorption peak. All data are expressed as "mean ± standard deviation (SD)".

3. Results and discussion

3.1 Characterization of prepared materials

A schematic of the preparation process of the CP-Lac@HOF-101 hydrogel was shown in Fig. 1a. Due to the stacking structure of layer-by-layer π···π, HOF-101 exhibited structural stability (Ma et al., 2020). The periodic carboxylate networks of HOF-101 could form hydrogen-bonded interactions between the surface residues of laccase, favoring the formation of a biointerface (Lin & Chen, 2019). Therefore, *in-situ* encapsulation of laccase in HOFs was highly advisable. Overall, the CMC and PVA hydrogel polymer composites as a supporter were obtained as supports via dissolution and cross-linking. Lac@HOF-101, as a biocatalyst, was mixed with PVA/CMC hydrogel and CP-Lac@HOF-101 gelation occurred via a simple freeze-thaw process in 1.0 M copper solutions. Lac@HOF-101, with needle-like crystals, was prepared using H4TBAPy as scaffold centers, and the 2-D periodic "square-frame-grid-lattices" was formed using carboxylic acid dimers as the self-assembled scaffold centers (Wied et al., 2022). Fig. 1(b, c) showed SEM images of Lac@HOF-101. CP-Lac@HOF-101 was shown to have a 3-D macroporous honeycomb network structure (Fig. 1d). HOFs easily attached to the hydroxyl groups of cellulose chains. Frozen samples were melted in 1.0 M copper solutions during the gelation process. The hydrogen bonds formed between the hydroxyl groups and water molecules

were expelled from the polymer chains, which led to aggregation of the polymer chains. As shown in Fig. 1e, CP-Lac@HOF-101 exhibited a rough surface, indicating that the Lac@HOF-101 was attached to the surface of the pore wall.

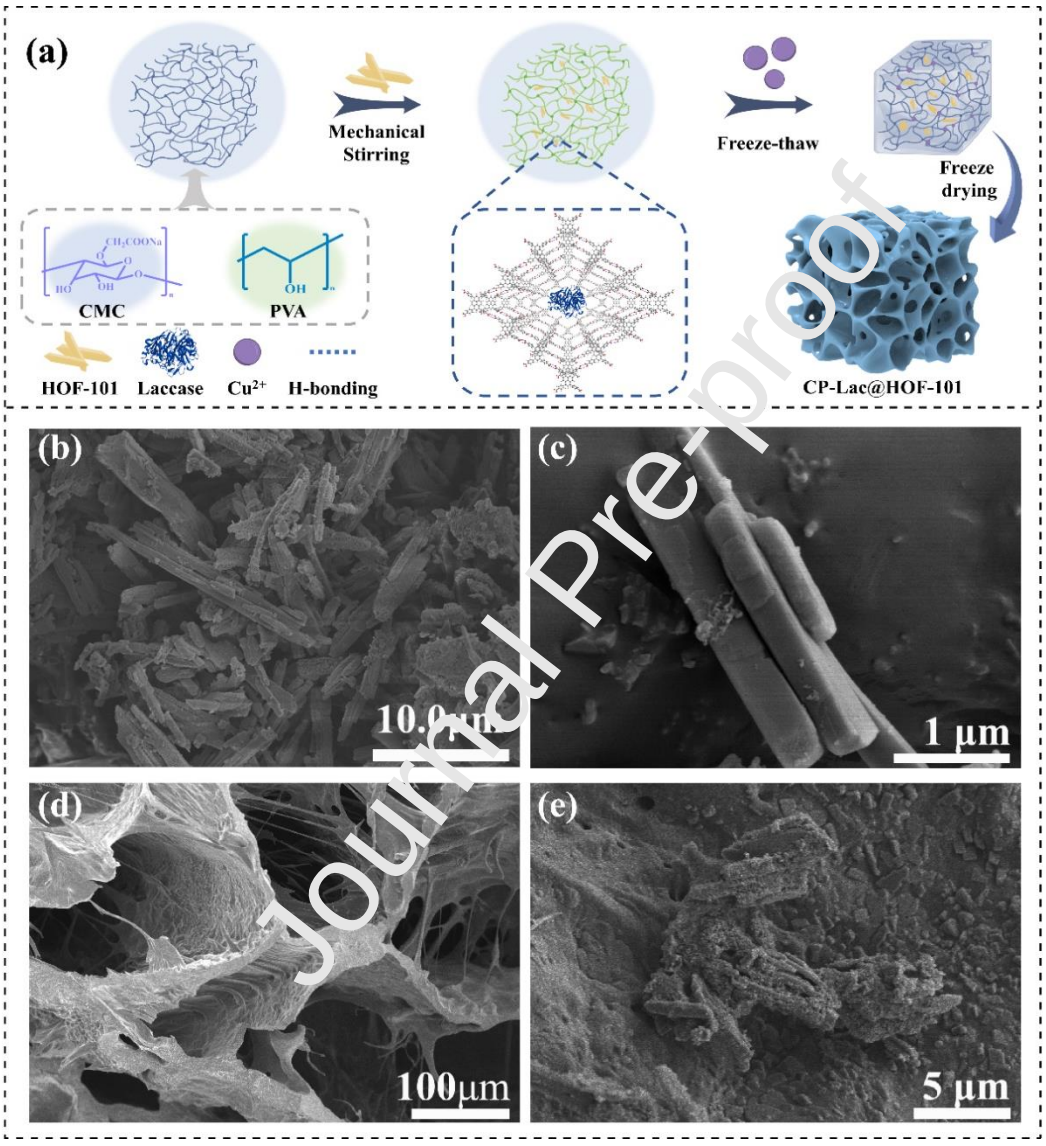

Fig. 1 (a) Schematic diagram of the preparation process of CP-Lac@HOF-101. SEM images of Lac@HOF-101 (b, c) and CP-Lac@HOF-101 (d, e) under different magnifications.

As shown in Fig. 2(a - d), the Bruner–Emmet–Teller (BET) surface area of CP-Lac@HOF-101 hydrogel was approximately 97.6 m^2/g, which was higher than CP hydrogel (88.1 m^2/g). Pore

size distribution analysis of CP-Lac@HOF-101 and CP revealed that their pore volumes were 0.28 and 0.23 cm^3/g, respectively. The higher surface area and pore volume of CP-Lac@HOF-101 were ascribed to porous HOFs. Therefore, the N_2 isotherm measurements indicated that HOFs were loaded into the CMC/PVA hydrogel. Based on the FT-IR spectrum (Fig. 2e), a typical amide I band of the protein appeared, demonstrating that laccase was successfully encapsulated in HOF-101. Furthermore, the stretching vibration peak of the amide I band in Lac@HOF-101 was slightly shifted owing to the H-bond interactions between the surface residues of laccase and the carboxylate networks (White, 2021). As shown in Fig. 2f, the energy dispersive spectroscopy (EDS) mapping of CP-Lac@HOF-101 showed that N was evenly distributed on the surface, demonstrating the encapsulation of laccase in the hydrogel.

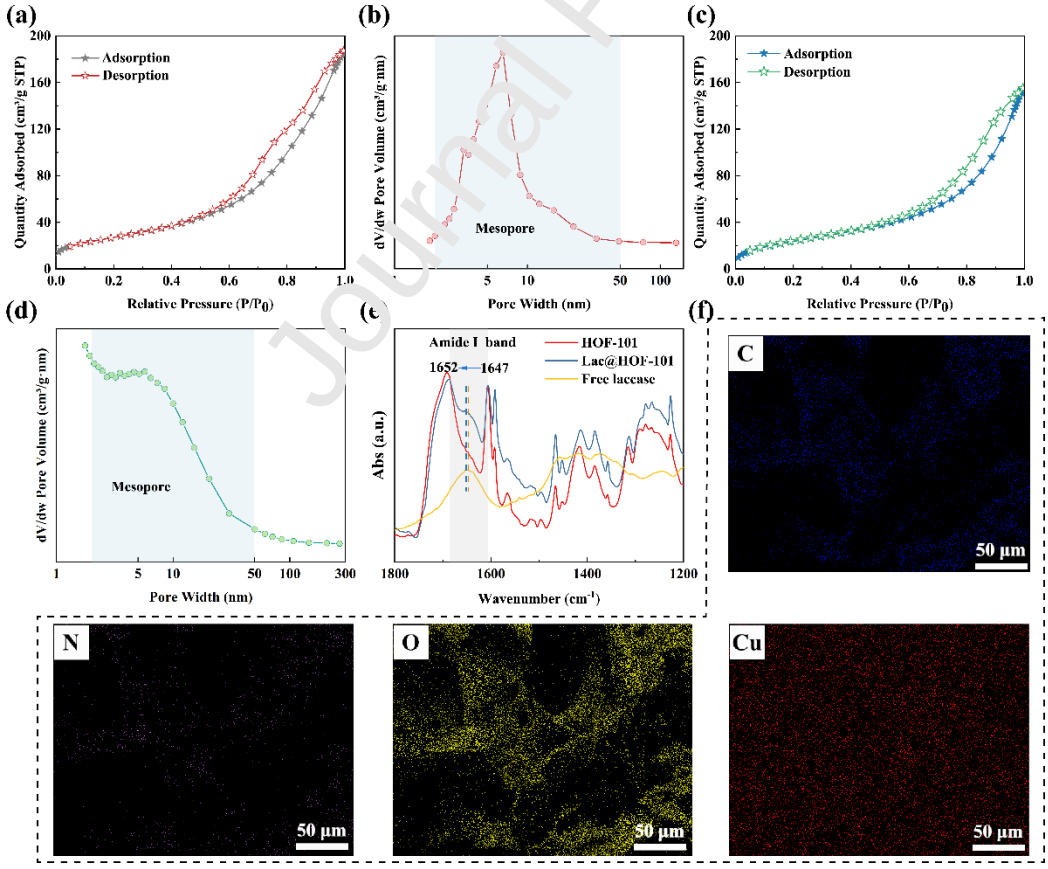

Fig. 2 The N_2 adsorption-desorption isotherm of CP (a, b) and CP-Lac@HOF-101 (c, d). EDS elemental maps of C, N, and O of Cu of CP-Lac@HOF-101 (f).

X-ray photoelectron spectroscopy (XPS) measurements were performed to determine the chemical structures of CP and CP-Lac@HOF-101. As shown in Fig. 3a, the survey spectrum of CP-Lac@HOF-101 exhibited distinctive peaks of Cu, C, N, and O, and the results were in line with the EDS characterization. Notably, the C content of CP-Lac@HOF-101 significantly increased. As shown in the high-resolution spectra of CP and CP-HOF-101 (Fig. 3b), the characteristic peaks at ~288.7, ~286.4 and 284.8 eV were attributed to C=O, C-O, and C-H/C-C, respectively. The binding energies of C-O shifted to a lower binding energy, illustrating that the intensity of the intermolecular hydrogen bonds visibly increased, leading to strong molecular interactions in CMC/PVA with HOFs (C. Yang, H.-R. Yang, Q.-D. An, Z.-Y. Xiao, & S.-R. Zhai, 2022). To gain further insight into the chemical structures of the samples, high-resolution O 1s XPS spectra were performed (Fig. 3c). The high-resolution O 1s peak was related to the Cu-O and C=C bands at 531.8 eV. The characteristic peaks at ~532.8 and ~534.2 eV corresponded to C-O/OH and C-O, respectively, confirming the structure of the CMC/PVA hydrogel. From the deconvolution results of Cu 2p shown in Fig. 3d, two dominant peaks were located at ~933.5 and 935.1 eV for CP and CP-Lac@HOF-101, which were assigned to Cu^{+} and Cu^{2+} species, respectively, indicating the coexistence of various metal species of $Cu^{+}/^{2+}$ (D. Wang, Lou, et al., 2021). The formation mechanism of CP-Lac@HOF-101 was shown in Fig. 3e. A 3-D macroporous honeycomb network was formed via double-cross-linked networks between CMC and PVA. The carboxyl and hydroxyl groups of the CMC/PVA to $Cu^{+}/^{2+}$ were spontaneously

bounded, and the hydroxyl groups of the hydrogels were attached to the HOFs.

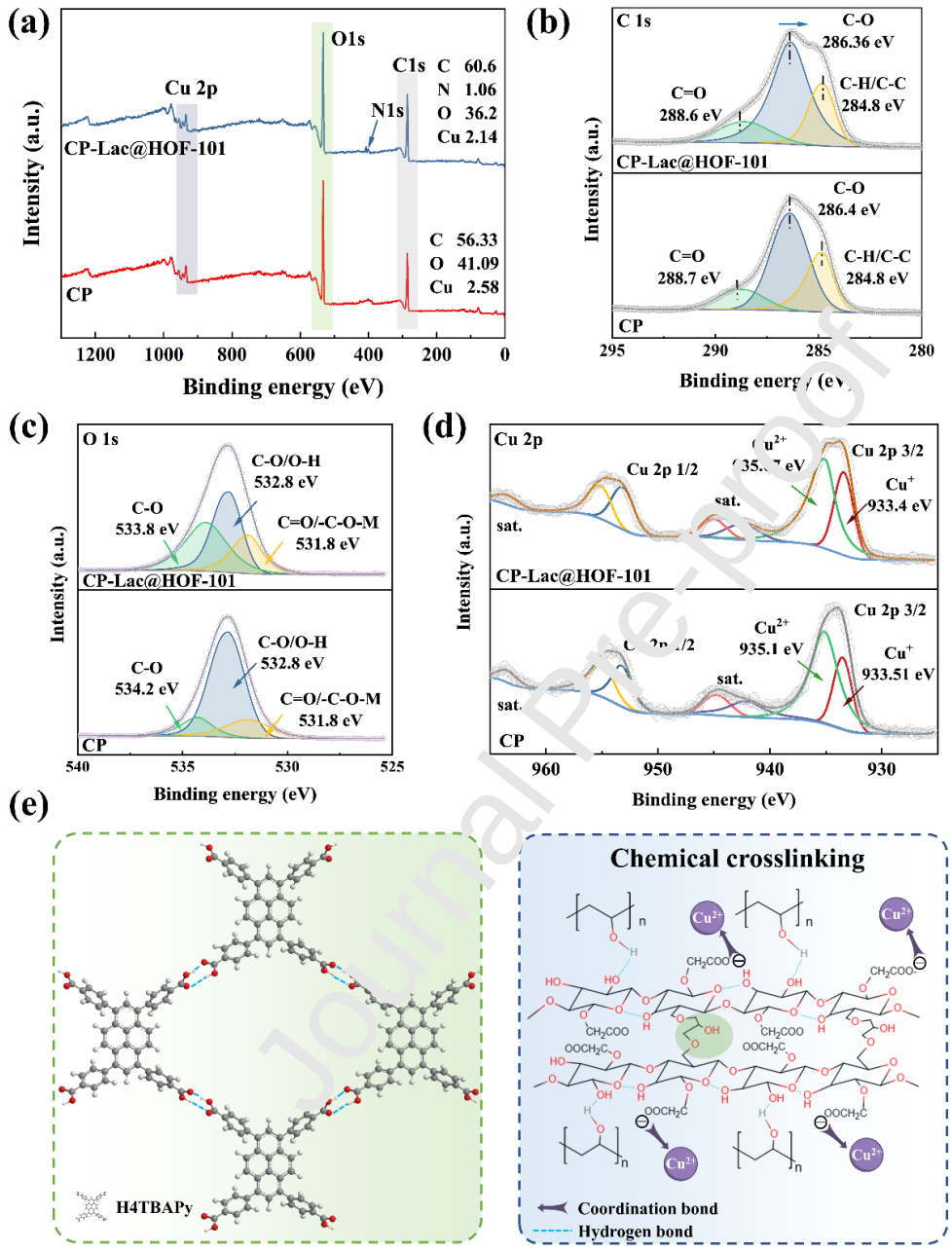

Fig. 3 XPS spectra of the prepared CP and CP-Lac@HOF-101 (a). High-resolution C 1s (b), O 1s (c), and Cu 2p of CP and CP-Lac@HOF-101. Formation mechanism of CP-Lac@HOF-101(e).

3.2. Biochemical characterization

3.2.1. Optimal pH and temperature

As shown in Fig. 4a, free and immobilized laccases reached their maximum activities at pH 4.0. This result showed that the laccase microenvironment did not change on the surface of the support and did not involve electrostatic interactions between laccase and the carrier (Lu, Zhao, & Wang, 2007). CP-Lac@HOF-101 retained 93.6 % of its maximum activity at pH 3.0, much higher than free laccase and the laccase immobilized on CMC/PVA hydrogel. However, with continuously increasing pH, the activities of the free and immobilized laccases decreased, because binding between the hydroxide anion and the active site of laccase hinders laccase-catalyzed reactions (Lassouane, Aït-Amar, Amrani, & Rodriguez-Couto, 2019). The activity of CP-Lac@HOF-101 remained above 50 % at pH 6.0, whereas that of laccase immobilized on CMC/PVA hydrogel decreased to 37.3 %. These results demonstrate the superiority of HOFs; the net-carboxylate-arranged cage could provide a highly hydrophilic and stable microenvironment for laccase.

As shown in Fig. 4b, the influence of temperature on free laccase, CP-Lac, and CP-Lac@HOF-101 was investigated in the range of 20 ℃–70 ℃ with a 10 ℃ interval. Immobilized laccase showed a higher optimum temperature than free laccase. The enzymes were slightly inhibited after encapsulation, and the steric hindrance was reduced by appropriately increasing the temperature (Zhang et al., 2020). The long-ordered channels of HOF-101 could exclude interferents and reduce molecular mobility to protect laccase (Chen et al., 2022). Therefore, Lac@HOF-101 could perform catalytic tasks in harsh environments. When the temperature reached 70 ℃, the free laccase was completely inactivated. Notably, the activity of

CP-Lac@HOF-101 remained above 35.0 %. For CP-Lac, the conformation of the enzymes was also stable owing to the hydrogen bonds between the CMC/PVA hydrogel and laccase (Huber et al., 2017); its activity remained at 13.2 %. Therefore, Lac@HOF-101 extended the pH and temperature ranges of laccase.

3.2.2. Thermal stability

Thermal stability was a critical part of immobilized enzymes. Thus, the activities of free and immobilized laccases were measured after heating at 50 ℃ for 3 h to assess the thermal stability. As shown in Fig. 4c, free laccase retained only 32.1 % of its initial activity after 3 h because the protein was denatured and inactivated by the high temperature. However, the thermal stability of the laccase improved after immobilization, especially for CP-Lac@HOF-101. CP-Lac@HOF-101 remained at 70.1 % of its initial activity after 3 h, which was higher than CP-Lac (62.4 %). This suggests that enzyme carriers could limit conformational changes in the protein structure. The HOFs further confined the laccase microenvironment, thereby enhancing its thermal durability.

3.2.3. Reusability of CP-Lac and CP-Lac@HOF-101

The reusability of the immobilized laccase was analyzed via recycling experiments using CP-Lac and CP-Lac@HOF-101. Remarkably, the activity of CP-Lac@HOF-101 was decreased by only 8.0 % in the first cycle of reusability tests (Fig. 4d). In case of CP-Lac, laccase was readily released from the CMC/PVA hydrogel. CP-Lac retained 89.1 % of its initial activity after the first cycle. Despite the fact that the relative activities of both CP-Lac and CP-Lac@HOF-101 were decreased because of inactivation or leaching of laccase during the catalytic cycle,

CP-Lac@HOF-101 retained 66.7 % of its initial activity after the fifth cycle. CP-Lac also exhibited similar stability, but its activity decreased to 30.7 % in the last cycle. More importantly, CP-Lac@HOF-101 retained 46.1 % of its initial activity during the last cycle. Above all, the net-carboxylate-arranged cage of HOFs and carrier of the CMC/PVA hydrogel offered protection to laccase to withstand harsh environments.

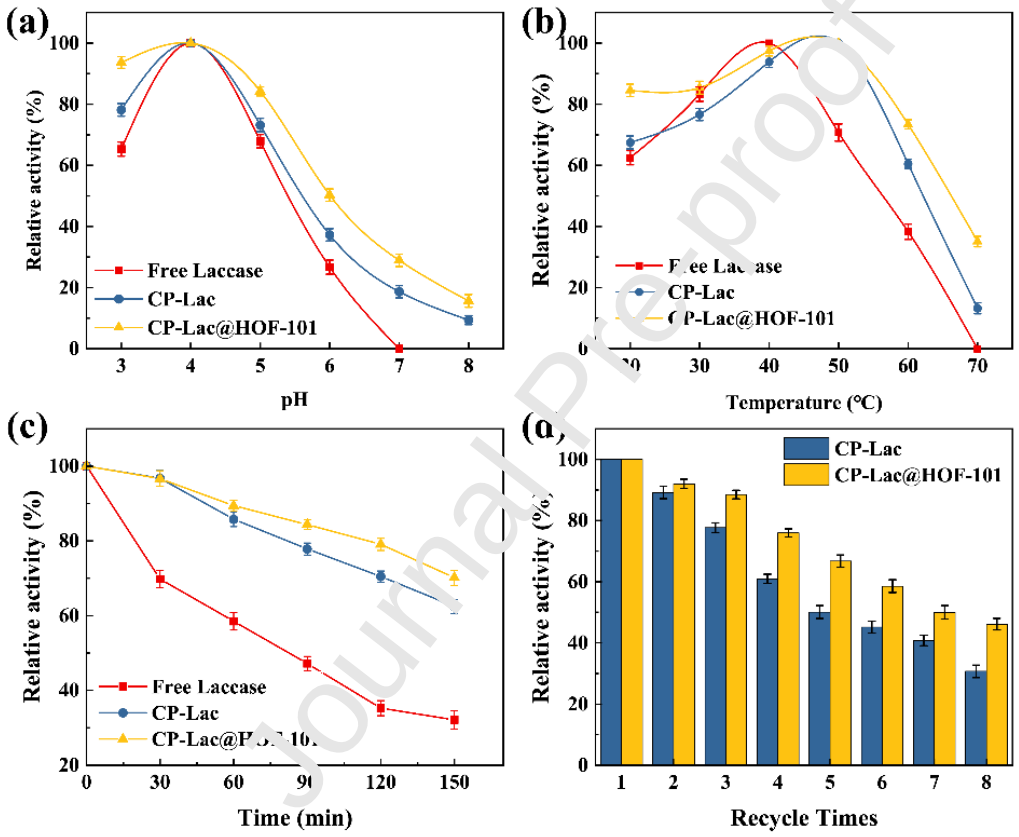

Fig. 4 Effect of pH (a) and temperature (b) on the activity of the free laccase, CP-Lac, and CP-Lac@HOF-101. The thermal stability (c) of the free laccase, CP-Lac, and CP-Lac@HOF-101. The operational stability of CP-Lac and CP-Lac@HOF-101 (d).

3.3. Decolorization of AO

To investigate the dye decolorization properties of CP-Lac@HOF-101, the azo dyes AO was

selected as the model pollutant. As shown in Fig. 5(a - c), the initial concentration of AO had a notable effect on decolorization by CP, CP-Lac, and CP-Lac@HOF-101. For the CP hydrogel, the decolorization rate gradually decreased with increasing AO concentration. The CP hydrogel exhibited fast adsorption during the initial 1 h, followed by a much slower adsorption, and subsequently, the adsorption achieved a balance for AO. The dye molecules were rapidly adsorbed onto the CP hydrogel surface and then slowly transferred and diffused into the pores of the hydrogel. Therefore, the initial concentration of the azo dyes greatly influences the removal efficiency of the honeycomb network structure hydrogel (Jiang et al., 2021).

Conversely, the decolorization rates of CP-Lac and CP-Lac@HOF-101 gradually increased with increasing AO concentrations (10 mg/L to 30 mg/L). The catalytic action of laccase, and not its adsorptive action, played a leading role in the decolorization process. When the initial concentration of the AO was too low, it was difficult for the substrate to contact immobilized laccase. When the concentration of AO reached 30 mg/L, the CP-Lac and CP-Lac@HOF-101 exhibited the maximum decolorization efficiencies of 57.7 % and 67.6 %, respectively. Remarkably, the decolorization rate for Lac@HOF-101 reached 67.1 % after 5 h when the concentration of AO increased to 50 mg/L. Meanwhile, the decolorization rate by CP-Lac also reached 55.4 %. The cupric ion cooperated with the substrate and active site of laccase, which increased the redox potential of laccase (Muthuvelu, Rajarathinam, Selvaraj, & Rajendren, 2020). The porous HOFs further accelerated the aggregation of the azo dyes, which shortened the contact time between the dyes and laccase. Therefore, the AO accumulated on Lac@HOF-101 and was degraded.

To investigate the adsorption process, the adsorption kinetics of AO onto CP, CP-Lac, and CP-Lac@HOF-101 were evaluated, as shown in Fig. 5(d, e) and Tab. 1. The first- and second-order kinetic models were expressed as follows:

$$Ln(q_e - q_t) = Lnq_e - k_1 t \quad (1)$$

$$\frac{t}{q_t} = \frac{1}{k_2 q_e^2} + \frac{t}{q_e} \quad (2)$$

where q_e and q_t were the adsorption capacities ($mg \cdot g^{-1}$) at equilibrium and at time t (min), k_1 (min^{-1}), and k_2 ($g\ mg^{-1}\ min^{-1}$) were the rates constant of first- and second-order adsorption, respectively. The second-order kinetic regression coefficients (R^2) of CP, CP-Lac, and CP-Lac@HOF-101 for AO were greater than 0.99 and more fitted than the pseudo-first-order models. The adsorption behavior could be better described by a pseudo-second-order kinetic model, which illustrates that the interactions between the AO molecules and the samples were controlled by chemisorption mechanisms (Pourhakkak, Taghizadeh, Taghizadeh, Ghaedi, & Haghdoust, 2021). Combined with the second-order kinetic model, the highest apparent reaction rate constant (k) of 0.06135 /min was obtained for CP, which was greater than those for CP-Lac (0.05768 /min) and CP-Lac@HOF-101 (0.04765 /min). This phenomenon may be caused by the spatial diffusion-limiting effect, as the immobilization carrier lowers the enzyme's protein flexibility (Liang et al., 2021). Notably, the decolorization efficiency of CP-Lac@HOF-101 was 67.6 % for 30 mg/L AO, which was much higher than that of CP hydrogel (54.4 %). Therefore, the combined action of efficient adsorption and enzymatic reactions improves the degradation efficiency of the azo dyes.

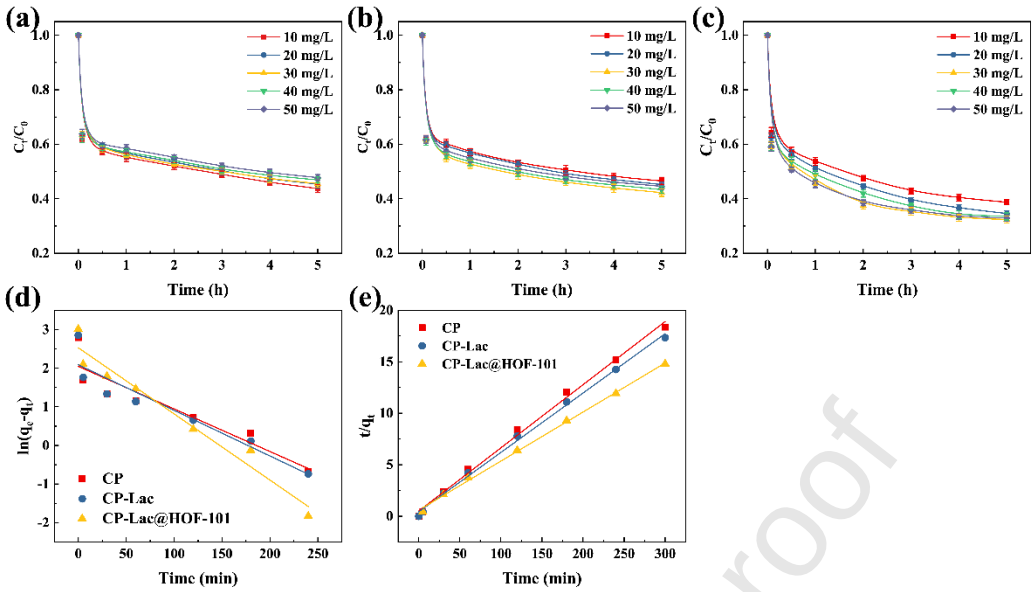

Fig. 5 Decolorization of AO by CP (a), CP-Lac (b), and CP-Lac@HOF-101 (c) with diverse initial dyes concentration. The first-order adsorption kinetic (d) and second-order adsorption kinetic (e) of samples for AO.

Table 1. Parameters of pseudo-first-order and pseudo-second-order kinetics.

	Pseudo-first-order model		Pseudo-second-order model	
	K_1	R^2	K_2	R^2
CP	-0.01103	0.84685	0.06135	0.99538
CP-Lac	-0.01181	0.86701	0.05768	0.99674
CP-Lac@HOF-101	-0.01713	0.95054	0.04765	0.99776

To investigate the practical applications of CP, CP-Lac, and CP-Lac@HOF-101, the influence of various environmental parameters on the decolorization process was investigated, and the results were shown in Fig. 6. The influence of temperature on the decolorization efficiency of free laccase, CP, CP-Lac, and CP-Lac@HOF-101 was investigated over the range of 20 °C–60 °C

within 5 h. As shown in Fig. 6a, temperature variation significantly influenced the degradation of AO. For free laccase, relatively high decolorization efficiencies were achieved at 30 °C–40 °C. As the environmental temperature increased, the protein gradually denatured until inactivation, thereby reducing decolorization efficiency. The decolorization efficiency of CP-Lac was enhanced by 18.6 % than that of CP hydrogel at 50 ℃, indicating that the synergistic system achieved a higher decolorization efficiency. The decolorization efficiency of CP-Lac@HOF-101 was further improved to 82.8 % than that of CP-Lac. The HOFs protected and stabilized laccase under harsh conditions, and the porous structures of the HOFs provided more adsorption sites for AO. The adsorption performance of CMC/PVA hydrogel improved with the temperature increase from 20 °C to 40 °C. The increase in the decolorization efficiency suggests that the AO molecules exhibited a positive movement of adsorption with increasing temperature. As the temperature continued to increase, the adsorption performance of the CMC/PVA hydrogel decreased slightly. The 3-D macroporous honeycomb network of the CMC/PVA hydrogel narrowed because the polymer chain assembled and shrank (Durán-Guerrero et al., 2018). Overall, when the temperature reached 40 °C, the decolorization efficiencies of free laccase and CP-Lac@HOF-101 were 37.4 % and 82.5 %, respectively. Although the adsorption and degradation capacity of CP-Lac@HOF-101 reduced at 60 °C, the efficiency remained above 74.8 %. Therefore, CP-Lac@HOF-101 exhibited outstanding performance over a wide temperature range, which was practical for water treatment.

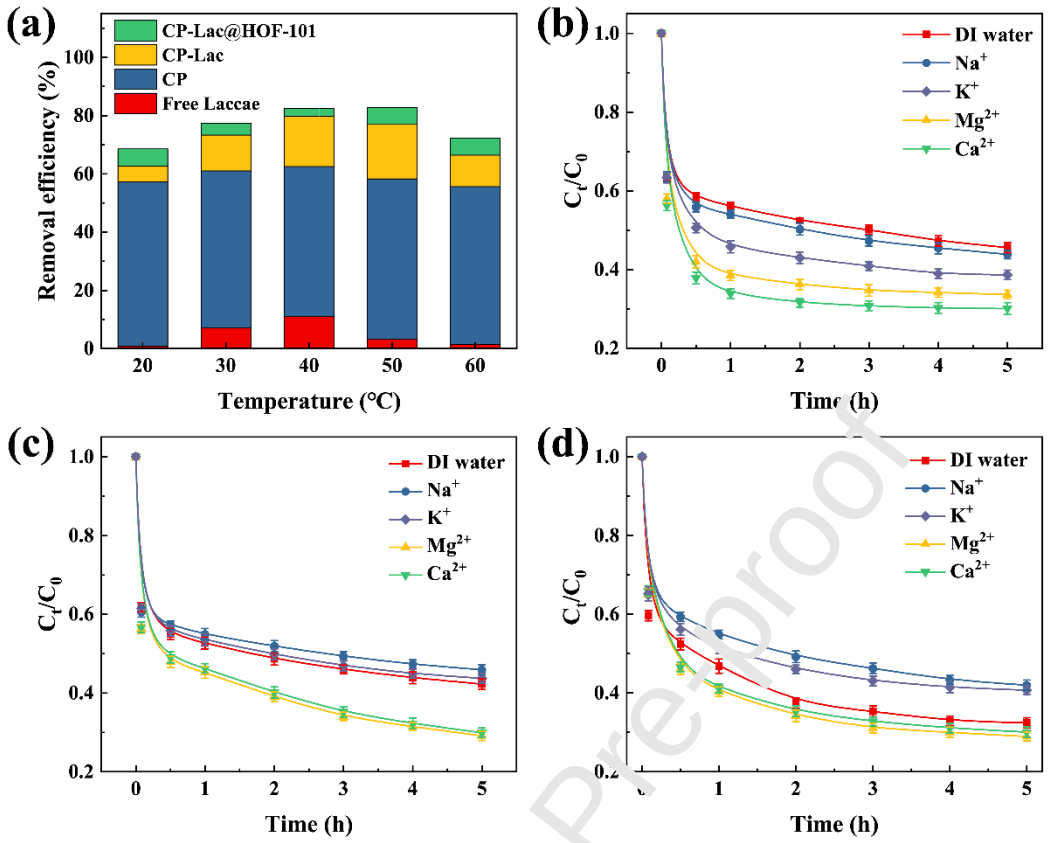

Fig. 6 The removal efficiency of AO by free laccase, CP-Lac and CP-Lac@HOF-101(a). Effects of various cations on the decolorization of AO with CP (b), CP-Lac (c) and CP-Lac@HOF-101(d).

Moreover, many different metal ions in authentic aquatic environments could decrease the decolorization abilities of CP, CP-Lac, and CP-Lac@HOF-101. The effects of coexisting K^+, Na^+, Mg^{2+}, and Ca^{2+} on the decolorization process was shown in Fig. 6(b - d). For the CMC/PVA hydrogel, AO adsorption was promoted to varying degrees in the presence of cations. In the presence of K^+ and Na^+, the adsorption of AO increased slightly because of the "salting-out" effect and hydrophobic interaction between the AO molecules and CMC/PVA hydrogel (Wu et al., 2021). For CP-Lac and CP-Lac@HOF-101, decolorization efficiency was inhibited in the

presence of K^+ and Na^+ (Fig. 6c, d). Enzyme activity was inhibited by competition between the electron transport system of laccase and monovalent metal ions in the surrounding environment (Murugesan, Kim, Jeon, & Chang, 2009). Therefore, adsorption played a pivotal role in the decolorization process in the presence of monovalent metal ions.

Furthermore, the divalent metal ions indirectly facilitated the adsorption of AO molecules via "cation bridging" between the CMC/PVA hydrogel. The decolorization efficiency was improved to 69.9 % in the presence of Ca^{2+}. CP-Lac and CP-Lac@HOF-101 exhibited significantly higher decolorization rates in the presence of Mg^{2+} and Ca^{2+}. This result could be attributed to the cooperative relationship between the divalent metal ions and the electron transport system of laccase. Divalent metal ions metallize HOFs, further improving the adsorption capacity of CP-Lac@HOF-101 (Xu, Wang, & Yan, 2021). The decolorization efficiency of CP-Lac@HOF-101 was 71.1 % in the presence of Ca^{2+}. Lac@HOF-101 exhibited excellent decolorization efficiency in complex water systems, illustrating that the synergetic system of adsorption and biocatalysis has broad prospects for practical water treatment applications.

The decolorization efficiencies of the dye solution by free laccase and laccase immobilized on different carriers were compared in Table 2. CP-Lac@HOF-101 exhibited the highest adsorption and degradation efficiencies. In this study, the high decolorization efficiency was caused by the synergistic effect between laccase catalysis and the "dual sorption effect" of CMC/PVA, and HOFs hydrogel composite showed great potential for wastewater purification.

Table 2 Comparison of decolorization efficiencies of the dye solution by laccase reported in the literature.

Method	Pollutant	Condition	Reaction time	Removal efficiency	Ref.
Bacterial laccase (*Bp*Lac) from *B. pumilus* ZB1	Remazol Brilliant Blue R	5 mg/L (Laccase-mediator system)	24 h	94.4 %	(Liu et al., 2023)
Laccase immobilized in vault nanoparticles	Acid Orange 7	50 mg/L	6 h	80.0 %	(Gao et al., 2022)
Biomimetic core-shell PDA@Lac bioreactor	Crystal violet	50 mg/L	24 h	Around 100.0 %	(Bo et al., 2023)
CP-Lac	acid orange 7	30 mg/L	5 h	79.7 %	This woke
CP-Lac@HOF-101	acid orange 7	30 mg/L	5 h	82.8 %	This woke

3.4 Mechanisms of adsorption and degradation

XPS characterization of the samples was performed after decolorization of AO to elucidate the adsorption and degradation mechanisms of CP and CP-Lac@HOF-101. As shown in Fig. 7a, all the elemental contents changed significantly after the decolorization process. The CMC/PVA hydrogel was proven to be an adsorptive platform for effectively capturing dye molecules from

wastewater. The main adsorption mechanism of the CMC/PVA hydrogels was further investigated. As shown in Fig. 7b, the percentage of C-O peak significantly enhanced after adsorption for AO (from 56.9 % to 63.2 %). The binding energy of the C-O peak shifted, indicating the occurrence of electrostatic attraction or hydrogen bonding (Xueping Li et al., 2022). Meanwhile, the C-O/O-H and C=O/C-O-M peaks were slightly shifted, which could contribute to the interaction between the oxygen vacancies and copper (II) coordination (Yu, Lou, Liu, & Zhou, 2020). Hence, it could be concluded that chelating and electrostatic interactions were produced between the oxygen atoms of AO and the metal ions. As shown in Fig. 7c, the valence state of the cupric ions did not change after adsorption. Furthermore, the binding energies of Cu^{+} and Cu^{2+} shifted to lower positions because of the coordination between the nitrogen-containing group and Cu^{+}/Cu^{2+}. In conclusion, the CMC/PVA hydrogel adsorbed dye molecules via chelation, electrostatic interactions, and hydrogen bonding.

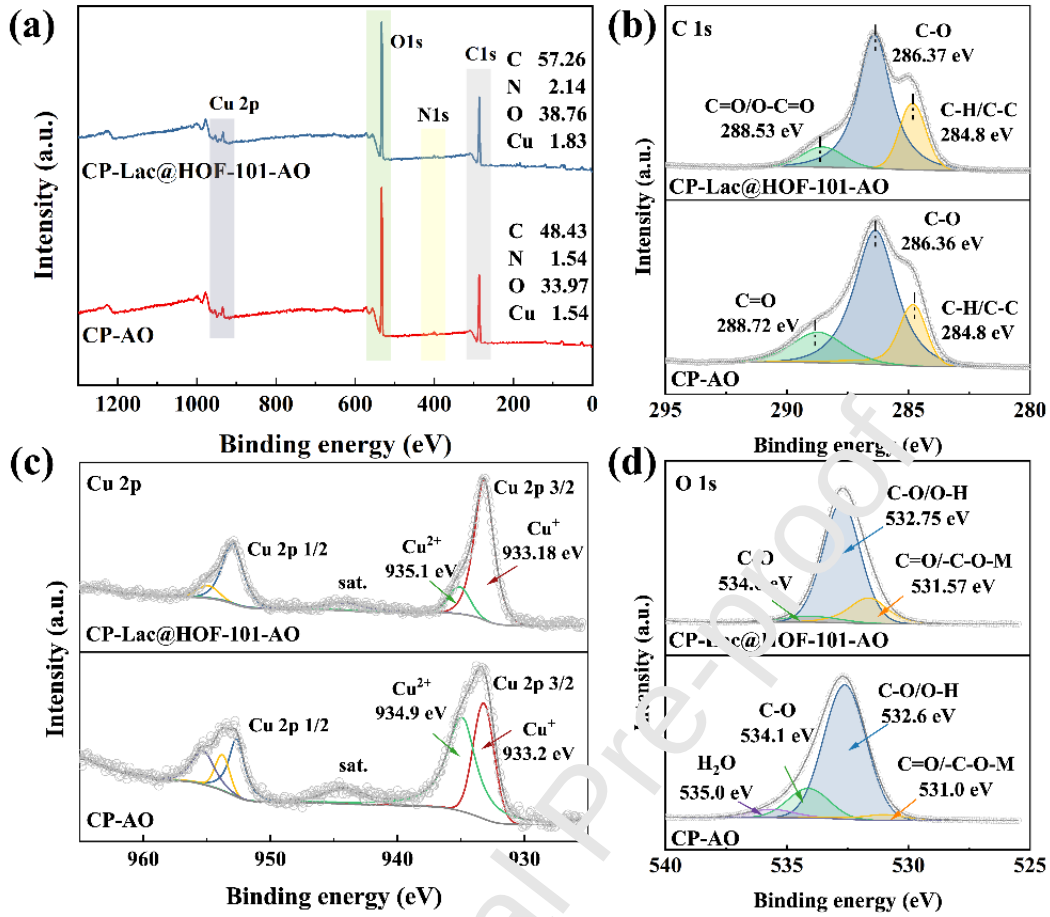

Fig.7 XPS spectra of CP-AO and CP-Lac@HOF-101-AO (a), the high-resolution C 1s (b), Cu2p (c) and O 1s (d) spectra fitting after AO adsorption.

The degradation mechanism of CP-Lac@HOF-101 was also explored. Decolorization of AO dyes with laccase occurred through the asymmetric cleavage of the -N=N- bond, and AO was further oxidized to form benzoic acid or fatty acids (Ramírez-Montoya, Hernández-Montoya, Montes-Morán, & Cervantes, 2015). The O 1s spectrum of CP-Lac@HOF-101-AO showed that the percentage of the C-O/O-H peak was significantly enhanced, confirming that benzoic acid or fatty acids were adsorbed on the CMC/PVA hydrogel. The degradation efficiency of the immobilized laccase increased significantly. This was because copper (II) acted as an activator

for laccase and assists in combining the substrate and active sites of the enzymes (Osipov et al., 2015). The XPS spectrum of Cu 2p of CP-Lac@HOF-101-AO showed that the relative content of Cu^{+} increased from 21.2 % to 50.1 %, whereas the content of Cu^{2+} correspondingly decreased. This also demonstrated that Cu^{+} could initiate the activation of laccase, and the higher specificity of Cu^{+} led to an increase in the redox potential, which could withdraw electrons from the substrate and increase the redox potential of laccase. The H-bonded network of HOF-101 may also facilitate proton transfer in laccase. Therefore, CP-Lac@HOF-101 exhibited higher biocatalyst accessibility. The adsorption and degradation mechanisms are shown in Fig. 8. CP-Lac@HOF-101 formed a synergistic system for adsorption and degradation that exhibited excellent decolorization efficiency in complex aquatic environments.

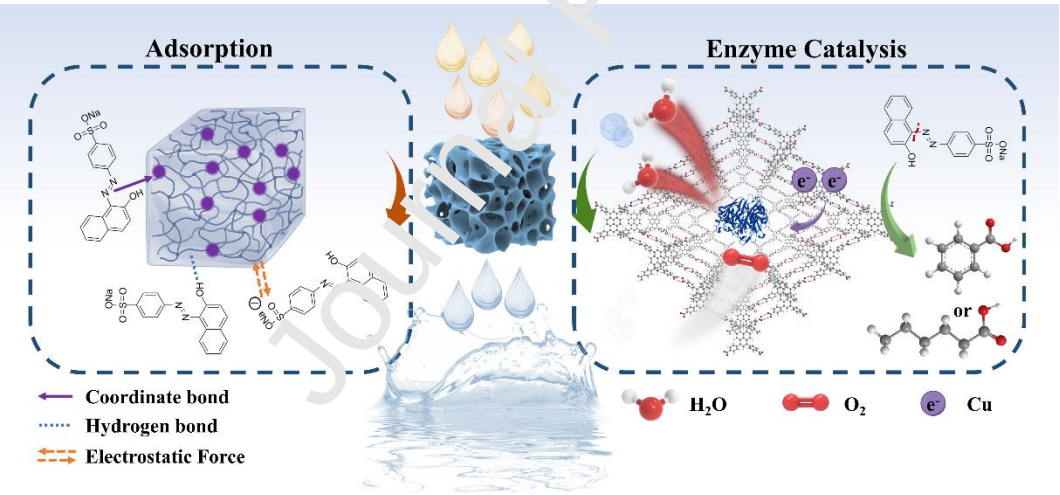

Fig. 8. Mechanism of adsorption and degradation for removing AO by CP-Lac@HOF-101.

Conclusion

In conclusion, HOF-101 was grown *in-situ* onto laccase via a mineralization process, and the

CP-Lac@HOF-101 hydrogel was successfully prepared using freeze–thaw cycles. The HOFs/hydrogel matrix exhibited good protection against laccase, which enhanced its environmental stability and reusability. Benefiting from the synergistic system of adsorption and catalytic degradation, CP-Lac@HOF-101 exhibited a high azo dyes removal efficiency. Lac@HOF-101 achieved 82.5 % of removal efficiency for AO within 5 h. Furthermore, CP-Lac@HOF-101 displayed outstanding tolerance to various metal ions during the decolorization process. This study provides a method for constructing enzyme@HOFs-based composite hydrogels and expanding the enzyme applications. The synergistic mechanism of the CP-Lac@HOF-101 system can guide future high-efficiency wastewater treatment strategies.

Acknowledgments

We thank the financial support from the National Natural Science Foundation of China (Grant No. 52003108), the China Postdoctoral Science Foundation funded project (2022M721359), the Fundamental Research Funds for the Central Universities (JUSRP121027) and the Postgraduate Research & Practice Innovation Program of Jiangsu Province (KYCX23_2476).

Disclosure statement

No potential conflict of interest was reported by the authors.

References

Backes, E., Kato, C. G., Corrêa, R. C. G., Moreira, R. d. F. P. M., Peralta, R. A., Barros, L., et al. (2021). Laccases in food processing: Current status, bottlenecks and perspectives. *Trends in Food Science & Technology,* 115, 445-460.

Bo, H., Zhang, Z., Chen, Z., Qiao, W., Jing, S., Dou, T., et al. (2023). Construction of a

biomimetic core-shell PDA@ Lac bioreactor from intracellular laccase as a nano-confined biocatalyst for decolorization. *Chemosphere*, 138654.

Bokare, A. D., Chikate, R. C., Rode, C. V., & Paknikar, K. M. (2008). Iron-nickel bimetallic nanoparticles for reductive degradation of azo dye Orange G in aqueous solution. *Applied Catalysis B: Environmental*, 79(3), 270-278.

Chen, G., Huang, S., Shen, Y., Kou, X., Ma, X., Huang, S., et al. (2021). Protein-directed, hydrogen-bonded biohybrid framework. *Chem*, 7(10), 2722-2742.

Chen, G., Tong, L., Huang, S., Huang, S., Zhu, F., & Ouyang, G. (2022). Hydrogen-bonded organic framework biomimetic entrapment allowing non-native biocatalytic activity in enzyme. *Nature Communications*, 13(1), 4816.

Dong, J., Wee, V., Peh, S. B., & Zhao, D. (2021). Molecular-Rotor-Driven Advanced Porous Materials. *Angewandte Chemie International Edition*, 60(30), 16279-16292.

Durán-Guerrero, J., Martínez Rodríguez, M., Garza-Navarro, M., Gonzalez-Gonzalez, V., Torres-Castro, A., & De La Rosa, J. R. (2018). Magnetic nanofibrous materials based on CMC/PVA polymeric blends. *Carbohydrate polymers*, 200, 289-296.

Feng, Y., Xu, Y., Liu, S., Wu, D., Su, Z., Chen, G., et al. (2022). Recent advances in enzyme immobilization based on novel porous framework materials and its applications in biosensing. *Coordination Chemistry Reviews*, 459, 214414.

Gao, Y. F., Wang, M., Shah, K., Kalra, S. S., Rome, L. H., & Mahendra, S. (2022). Decolorization and detoxification of synthetic dye compounds by laccase immobilized in vault nanoparticles. *Bioresource Technology*, 351.

Ghaheh, F. S., Taghizadeh, M., Taghizadeh, A., Hayati, B., Mahmoodi, N. M., & Parastar, S. (2021). Clean synthesis of rock candy-like metal–organic framework biocomposite for toxic contaminants remediation. *Environmental Technology & Innovation*, 23, 101747.

Hasan, M. N., Shenashen, M., Hasan, M. M., Znad, H., & Awual, M. R. (2021). Assessing of cesium removal from wastewater using functionalized wood cellulosic adsorbent. *Chemosphere*, 270, 128668.

Huang, S., Chen, G., & Ouyang, G. (2022). Confining enzymes in porous organic frameworks: from synthetic strategy and characterization to healthcare applications. *Chemical Society Reviews*, 51(15), 6824-6863.

Huber, D., Tegl, G., Baumann, M., Sommer, E., Gorji, E. G., Borth, N., et al. (2017). Chitosan hydrogel formation using laccase activated phenolics as cross-linkers. *Carbohydrate polymers*, 157, 814-822.

Iark, D., dos Reis Buzzo, A. J., Garcia, J. A. A., Côrrea, V. G., Helm, C. V., Corrêa, R. C. G., et al. (2019). Enzymatic degradation and detoxification of azo dye Congo red by a new laccase from Oudemansiella canarii. *Bioresource technology*, 289, 121655.

Javanbakht, S., Pooresmaeil, M., & Namazi, H. (2019). Green one-pot synthesis of carboxymethylcellulose/Zn-based metal-organic framework/graphene oxide bio-nanocomposite as a nanocarrier for drug delivery system. *Carbohydrate Polymers*, 208, 294-301.

Jiang, R., Zhu, H.-Y., Fu, Y.-Q., Jiang, S.-T., Zong, E.-M., Zhu, J.-Q., et al. (2021). Colloidal CdS sensitized nano-ZnO/chitosan hydrogel with fast and efficient photocatalytic

removal of congo red under solar light irradiation. *International Journal of Biological Macromolecules,* 174, 52-60.

Kitagawa, S. (2017). Future porous materials. *Accounts of Chemical Research,* 50(3), 514-516.

Kurade, M. B., Waghmode, T. R., Patil, S. M., Jeon, B.-H., & Govindwar, S. P. (2017). Monitoring the gradual biodegradation of dyes in a simulated textile effluent and development of a novel triple layered fixed bed reactor using a bacterium-yeast consortium. *Chemical Engineering Journal,* 307, 1026-1036.

Lassouane, F., Aït-Amar, H., Amrani, S., & Rodriguez-Couto, S. (2019). A promising laccase immobilization approach for Bisphenol A removal from aqueous solutions. *Bioresource technology,* 271, 360-367.

Li, S., & Huo, F. (2015). Metal–organic framework composites: from fundamentals to applications. *Nanoscale,* 7(17), 7482-7501.

Li, X., Li, D., Zhang, Y., Lv, P., Feng, Q., & Wei, Q. (2020). Encapsulation of enzyme by metal-organic framework for single-enzymatic biofuel cell-based self-powered biosensor. *Nano Energy,* 68, 104308.

Li, X., Wu, Z., Tao, X., Li, R., Tian, D., & Liu, X. (2022). Gentle one-step co-precipitation to synthesize bimetallic CoCu-MOF immobilized laccase for boosting enzyme stability and Congo red removal. *Journal of Hazardous Materials,* 438, 129525.

Liang, W., Carraro, F., Solomon, M. B., Bell, S. G., Amenitsch, H., Sumby, C. J., et al. (2019). Enzyme encapsulation in a porous hydrogen-bonded organic framework. *Journal of the American Chemical Society,* 141(36), 14298-14305.

Liang, W., Wied, P., Carraro, F., Sumby, C. J., Nidetzky, B., Tsung, C.-K., et al. (2021). Metal–organic framework-based enzyme biocomposites. *Chemical Reviews*, 121(3), 1077-1129.

Lin, R.-B., & Chen, B. (2019). Of HOF hosts. *Nature Chemistry,* 11(12), 1078-1080.

Liu, J. S., Li, B. X., Li, Z., Yang, F., Chen, B. X., Chen, J. H., et al. (2023). Deciphering the alkaline stable mechanism of bacterial laccase from Bacillus pumilus by molecular dynamics simulation can improve the decolorization of textile dyes. *Journal of Hazardous Materials*, 443.

Lu, L., Zhao, M., & Wang, Y. (2007). Immobilization of laccase by alginate–chitosan microcapsules and its use in dye decolorization. *World Journal of Microbiology and Biotechnology*, 23, 159-166.

Ma, K., Li, P., Xin, J. H., Chen, Y., Chen, Z., Goswami, S., et al. (2020). Ultrastable mesoporous hydrogen-bonded organic framework-based fiber composites toward mustard gas detoxification. *Cell Reports Physical Science*, 1(2), 100024.

Malik, E. M., & Müller, C. E. (2016). Anthraquinones as pharmacological tools and drugs. *Medicinal research reviews,* 36(4), 705-748.

Miao, Q., Jiang, L., Yang, J., Hu, T., Shan, S., Su, H., et al. (2022). MOF/hydrogel composite-based adsorbents for water treatment: A review. *Journal of Water Process Engineering*, 50, 103348.

Murugesan, K., Kim, Y.-M., Jeon, J.-R., & Chang, Y.-S. (2009). Effect of metal ions on reactive dye decolorization by laccase from Ganoderma lucidum. *Journal of Hazardous Materials*, 168(1), 523-529.

Muthuvelu, K. S., Rajarathinam, R., Selvaraj, R. N., & Rajendren, V. B. (2020). A novel method for improving laccase activity by immobilization onto copper ferrite nanoparticles for lignin degradation. *International Journal of Biological Macromolecules,* 152, 1098-1107.

Osipov, E., Polyakov, K., Tikhonova, T., Kittl, R., Dorovatovskii, P., Shleev, S., et al. (2015). Incorporation of copper ions into crystals of T2 copper-depleted laccase from Botrytis aclada. *Acta Crystallographica Section F: Structural Biology Communications,* 71(12), 1465-1469.

Peng, J., Wu, E., Lou, X., Deng, Q., Hou, X., Lv, C., et al. (2021). Anthraquinone removal by a metal-organic framework/polyvinyl alcohol cryogel-immobilized laccase: Effect and mechanism exploration. *Chemical Engineering Journal,* 418, 129473.

Pierrat, É., Laurent, A., Dorber, M., Rygaard, M., Verones, F., & Hauschild, M. (2023). Advancing water footprint assessments: Combining the impacts of water pollution and scarcity. *Science of The Total Environment,* 870, 161910.

Pourhakkak, P., Taghizadeh, A., Taghizadeh, M., Ghaedi, M., & Haghdoust, S. (2021). *Fundamentals of adsorption technology*. In *Interface Science and Technology* (pp. 1-70): Elsevier

Rajoriya, S., Bargole, S., George, S., & Saharan, V. K. (2018). Treatment of textile dyeing industry effluent using hydrodynamic cavitation in combination with advanced oxidation reagents. *Journal of Hazardous Materials,* 344, 1109-1115.

Ramírez-Montoya, L. A., Hernández-Montoya, V., Montes-Morán, M. A., & Cervantes, F. J. (2015). Correlation between mesopore volume of carbon supports and the immobilization

of laccase from Trametes versicolor for the decolorization of Acid Orange 7. *Journal of Environmental Management*, 162, 206-214.

Slama, H. B., Chenari Bouket, A., Pourhassan, Z., Alenezi, F. N., Silini, A., Cherif-Silini, H., et al. (2021). Diversity of synthetic dyes from textile industries, discharge impacts and treatment methods. *Applied Sciences*, 11(14), 6255.

Solayman, H., Hossen, M. A., Abd Aziz, A., Yahya, N. Y., Hon, L. K., Ching, S. L., et al. (2023). Performance Evaluation Of Dye Wastewater Treatment Technologies: A Review. *Journal of Environmental Chemical Engineering*, 109610.

Su, J., Fu, J., Wang, Q., Silva, C., & Cavaco-Paulo, A. (2018). Laccase: a green catalyst for the biosynthesis of poly-phenols. *Critical Reviews in Biotechnology*, 38(2), 294-307.

Tang, J., Liu, J., Zheng, Q., Li, W., Sheng, J., Mao, L., et al. (2021). In-Situ Encapsulation of Protein into Nanoscale Hydrogen-Bonded Organic Frameworks for Intracellular Biocatalysis. *Angewandte Chemie*, 133(41), 22489-22495.

Wang, D., Lou, J., Yuan, J., Xu, J., Zhu, R., Wang, Q., et al. (2021). Laccase immobilization on core-shell magnetic metal-organic framework microspheres for alkylphenol ethoxylate compound removal. *Journal of Environmental Chemical Engineering*, 9(1), 105000.

Wang, D., Zhu, R., Lou, J., Yuan, J., Xu, J., & Fan, X. (2021). Novel marigold-like CuO@ Cu-based MOFs composite photocatalyst for high-performance removal of alkylphenol ethoxylate under visible light. *Journal of Environmental Chemical Engineering*, 9(6), 106434.

Wang, F., Guo, C., Yang, L.-r., & Liu, C.-Z. (2010). Magnetic mesoporous silica nanoparticles:

fabrication and their laccase immobilization performance. *Bioresource technology,* 101(23), 8931-8935.

White, N. G. (2021). Amidinium··· carboxylate frameworks: predictable, robust, water-stable hydrogen bonded materials. *Chemical communications,* 57(84), 10998-11008.

Wied, P., Carraro, F., Bolivar, J. M., Doonan, C. J., Falcaro, P., & Nidetzky, B. (2022). Combining a Genetically Engineered Oxidase with Hydrogen-Bonded Organic Frameworks (HOFs) for Highly Efficient Biocomposites. *Angewandte Chemie International Edition,* 61(16), e202117345.

Wu, S., Hua, M., Alsaid, Y., Du, Y., Ma, Y., Zhao, Y., et al. (2021). Poly (vinyl alcohol) hydrogels with broad-range tunable mechanical properties via the Hofmeister effect. *Advanced Materials,* 33(11), 2007829.

Xiao, X., Tu, S., Lu, M., Zhong, H., Zheng, C., Zuo, X., et al. (2016). Discussion on the reaction mechanism of the photocatalytic degradation of organic contaminants from a viewpoint of semiconductor photo-induced electrocatalysis. *Applied Catalysis B: Environmental,* 198, 124-132.

Xu, X., Wang, J., & Yan, B. (2021). Facile fabrication of luminescent Eu (III) functionalized HOF hydrogel film with multifunctionailities: quinolones fluorescent sensor and anticounterfeiting platform. *Advanced Functional Materials,* 31(37), 2103321.

Yang, C., Yang, H.-R., An, Q.-D., Xiao, Z.-Y., & Zhai, S.-R. (2022). Recyclable CMC/PVA/MIL-101 aerogels with tailored network and affinity sites for efficient heavy metal ions capture. *Chemical Engineering Journal,* 447, 137483.

Yang, C., Yang, H. R., An, Q. D., Xiao, Z. Y., & Zhai, S. R. (2022). Recyclable CMC/PVA/MIL-101 aerogels with tailored network and affinity sites for efficient heavy metal ions capture. *Chemical Engineering Journal*, 447.

Yang, H., Fu, J., Huang, W., Wu, T., Huang, S., Chen, G., et al. (2023). Self-Propelled, High-Crystalline Hydrogen-Bonded Enzymatic Framework Assembled by Bottom-Up Strategy. *Small Structures*, 2200346.

Yu, K., Lou, L. L., Liu, S., & Zhou, W. (2020). Asymmetric oxygen vacancies: the intrinsic redox active sites in metal oxide catalysts. *Advanced Science*, 7(2), 1901970.

Yuan, Y., Yin, W., Huang, Y., Feng, A., Chen, T., Qiao, L., et al. (2023). Intermittent electric field stimulated reduction-oxidation coupled process for enhanced azo dye biodegradation. *Chemical Engineering Journal*, 451, 138732.

Zhang, R., Wang, L., Han, J., Wu, J., Li, C., Ni, L., et al. (2020). Improving laccase activity and stability by HKUST-1 with cofactor via one-pot encapsulation and its application for degradation of bisphenol A. *Journal of Hazardous Materials*, 383, 121130.

CRediT Author statement

Xue Yang: Conceptualization, Methodology, Analysis, Writing-Original Draft.

Fei Shi: Editing, Methodology.

Xiaolei Su: Editing, Methodology.

Artur Cavaco-Paulo: Supervision, Resources.

Jing Su: Conceptualization, Supervision, Review & Editing, Project administration, Funding Acquisition.

Hongbo Wang: Supervision, Project administration.

Declaration of interests

☒ The authors declare that they have no known competing financial interests or personal relationships that could have appeared to influence the work reported in this paper.

☐The authors declare the following financial interests/personal relationships which may be considered as potential competing interests:

Graphical abstract